Defence Research and Development Canada
Recherche et développement pour la défense Canada

DEFENCE R&D DÉFENSE

Characterization of Nanoparticles by Capillary Electrophoresis and Trapping of Nanoparticles in Microfluidics Device

Final Report

T. Tang, A.B. Jemere and D.C.W. Mah, Projects Director
Canada West Biosciences Inc.

Contract Scientific Authority: W.E. Lee, DRDC Suffield

The scientific or technical validity of this Contract Report is entirely the responsibility of the contractor and the contents do not necessarily have the approval or endorsement of Defence R&D Canada.

Defence R&D Canada
Contract Report
DRDC Suffield CR 2009-177
August 2009

Canada

Characterization of Nanoparticles by Capillary Electrophoresis and Trapping of Nanoparticles in Microfluidics Device

Final Report

T. Tang, A.B. Jemere and D.C.W. Mah, Projects Director
Canada West Biosciences Inc.
5429-60th Street,
Camrose, AB, T4V 4G9

Contract Number: W7702-04R021/001/EDM

Contract Scientific Authority: W.E. Lee (403-544-4706)

The scientific or technical validity of this Contract Report is entirely the responsibility of the contractor and the contents do not necessarily have the approval or endorsement of Defence R&D Canada.

Defence R&D Canada – Suffield

Contract Report

DRDC Suffield CR 2009-177

August 2009

© Canada West Biosciences Inc., 2008

Abstract

The contractor report describes research performed for Contract No. W7702-04R-021. The work was carried out in support of CRTI 03-005RD. The report describes the use of capillary electrophoresis (CE) as an analytical method for characterizing gold, polymer and iron oxide nanoparticles (NPs). The analyte species were detected by UV/vis or laser-induced fluorescence (LIF) spectroscopy. For analytes that possessed neither UV/vis absorbance nor LIF, indirect methods of detection were employed whereby a signal-generating molecular species was added to the running buffer. NPs from a variety of commercial sources and from custom syntheses were studied. The report demonstrates that CE is a valuable tool in NP research. The report also demonstrates the feasibility of trapping nanoparticles in microfluidic devices for sample clean up and detection.

This page intentionally left blank.

Executive Summary

Introduction

The work in this contract report was carried out in support of CRTI project 03-0005RD. DRDC Suffield was a research partner in the project that was lead by Industrial Materials Institute-National Research Council Canada (Boucherville QC). Canada West Biosciences undertook research under contract to DRDC Suffield. The purpose of the contract was analytical chemical research support in areas of nanoparticles (NPs) and in design of micro-sized biological detection systems. To this end the physico-chemical properties of a variety of NPs were examined using capillary electrophoresis (CE). Methods of trapping nanoparticles in a microfluidic device were also examined.

Results: Analyses of NPs composed of polymer, gold or iron oxide were carried out to determine electrophoretic mobility, size distribution and charge/size ratio.

Significance: The work demonstrated that CE is a valuable tool in NP research. The physico-chemical properties of NPs have critical effects on their behaviour in bio-analytical devices. Thus NPs used in such devices must be subject to quality control and quality assurance (qc/qa). For a technology to advance from the experimental stage to the technology-demonstration model, chemical methods, reagents and other components need to be standardized. Analyses presented in this report have pointed the way to using CE in routine methods for qc/qa of NPs themselves and for microfluidic systems designed to trap NPs.

Future plans: CRTI project 03-0005RD was completed in 2007. Subsequent and future work on a technology demonstration for a microfluidic biological detection system is funded through a CRTI technology demonstration project. DRDC Suffield continues as a partner in the project (CRTI 06-0187TD) providing bio-analytical chemistry and microfluidic system design.

.

T. Tang, A.B. Jemere, D.C.W. Mah 2009 Capillary Electrophoresis of Nanoparticles
PWGS Canada W7702-04R021/001/EDM Canada West Biosciences

This page intentionally left blank.

Table of Contents

Abstract.. i

Executive Summary iii

Sommaire...iv

Table of Contents v

Acknowledgements vi

PART I. Characterization of Nanoparticles by Capillary Electrophoresis 1

1. Introduction...1
2. Experimental Section...2
    2.1 Chemicals and reagents...2
    2.2 CE analysis, microchip devices and fluorescence measurements..............................3
3. Results and Discussion 4
    3.1 Capillary electrophoresis of polymeric NPs using direct LIF detection 4
    3.2 Capillary electrophoresis of NPs using UV absorbance detection...................9
    3.3 Capillary electrophoresis of NPs using indirect LIF detection 10
4. Conclusions..14

PART II. Trapping Nanoparticles in Microfluidic Device 15

References...19

Acknowledgements

The authors would like to thank Dr William Lee at DRDC Suffield for the invaluable advice and understanding in consideration of this contract. We are also grateful to Dr Teodor Veres at Industrial Materials Institute (IMI-NRC) and Dr Neil Cameron for supplying the iron core nanoparticles.

Part I Characterization of Nanoparticles by Capillary Electrophoresis

1. Introduction

The work in this contract report was carried out in support of CRTI project 03-0005RD. DRDC Suffield was a research partner in the project that was lead by Industrial Materials Institute-National Research Council Canada (Boucherville QC). Canada West Biosciences undertook research under contract to DRDC Suffield.

Nanoparticles (NPs) continue to attract widespread attention in biomedical applications; immunolabelled magnetic particles are broadly used in cytometry, microbiology and molecular biology [1-2]. In recent years many methods have been introduced to synthesize metal nanoparticles (Au, Ag, Fe, etc) with one of the major goals being the manufacturing of NPs for sensor development [3-4]. Due to their large surface-to-volume ratio, NPs can be used as pseudo-stationary phases in analytical separations such as liquid chromatography and capillary electrochromatography [5]. Characterization and quantification of these submicron particles is a challenge because the size of a particle is an important factor in its physical properties. The most commonly used methods to determine size and size-distribution of NPs involve transmission electron microscopy (TEM) and size-exclusion chromatography [6]. These methods, however, have some inherent problems such as degradation of samples and irreversible adsorption of surface-active NPs. TEM is often time consuming and by itself does not offer any separation capability. Faster analysis methods that provide insight into size and surface properties would be useful to NP research.

Capillary electrophoresis (CE) is a well established powerful separation technique for the separation of charged molecules according to their size-to-charge ratio. CE is not limited to the separation of molecules but also to that of charged particulate materials. CE offers a number of advantages, including speed, autosampling, and requirement of minute amounts of samples. Recently, CE has been applied to the separation of a variety of different size materials, including inorganic oxide, latex, polystyrene, silicate, gold and silver NPs [7-11]. In CE, ions are separated in a free-flow, open tubular mode driven by electroosmotic flow and the inherent electrophoretic mobility of the analytes under the influence of an applied electric field. For example, gold NPs are charged due to sorption of ions onto their surfaces during the synthesis process, which subsequently results in the formation of an electrical double layer [12].

In the CRTI project, NPs were grafted with DNA probes so that target DNA molecules could be purified, concentrated and detected in microfluidic devices, using electromagnetic traps or physical barriers, with high sensitivity, specificity and speed. Understanding the surface charge properties and size distribution of these in-house made NPs is important. As part of the consulting support the DRDC-Suffield team made preliminary studies on the use of capillary electrophoresis to characterize NPs by size using laser induced fluorescence and absorbance detection methods.

2. Experimental Section

2.1 Chemicals and reagents

Tris(hydroxymethyl)aminomethane (Tris) and thiourea were purchased from Sigma-Aldrich Canada Ltd. (Oakville, ON). 2-(N-Morpholino)ethane sulphonic acid (MES) was from ICN Biomedical Inc. (Aurora, OH). BODIPY 493/503 (4,4-difluro-1,3,5,7,8-penta methyl-4-bora-3a,4a-diaza-s-indacene) and fluorescein were from Molecular Probes (Eugene, OR), and were prepared as a 0.1 mM stock solution in HPLC grade methanol (Fisher, Fair Lawn, NJ) and in ultra pure water, respectively. 55 nm and 210 nm polymeric nanoparticles, labeled with Dragon green (interior) and fluorescein (exterior), respectively, were purchased from Bangs Laboratories (Fishers, IN, USA). The 55 nm particles were obtained in DI water that contained 0.1% Tween 20 and the 210 nm particles were obtained in DI water that contained 0.5% HEPES and 0.1% Tween 20. Lucifer yellow-labeled 1 μm beads, Fe_3O_4@NMe_4OH and 200 nm $Fe_3O_4SiO_2$ particles were prepared by Industrial Materials Institute (Boucherville, QC). Lucifer yellow dye was provided by IMI (Montreal, QC). Au NPs, were purchased from Sigma-Aldrich (5 nm and 20 nm dia) or kindly provided by Dr David Pedersen (DRDC Suffield) (approximately 10 nm dia.). Buffers were prepared using ultra pure water prepared with a deionizing system (Millipore Canada, Mississauga, ON) from distilled water, and filtered through a nylon syringe filter (0.2 µm pore size, Nalgene, Rochester, NY) prior to use.

2.2 CE analysis, microchip devices and fluorescence measurements

CE-LIF studies were performed using a Beckman 5010 CE instrument (Beckman Coulter Inc., Fullerton, CA) equipped with an argon ion laser operated at 488 nm excitation and 520 nm emission. UV-Absorbance measurements were made at 214 nm. Samples were run on a 37 cm or 47 cm long, 50 µm id. fused silica capillary from PolyMicro Technologies (Phoenix, Az, USA) at column temperature of 25 ^oC. Prior to sample run, the capillary was conditioned with 0.1 M NaOH for 10 minutes, water for 5 minutes followed by equilibration with the separation buffer for 30 minutes. In between runs, the capillary was conditioned with 0.1 M NaOH for 2 minutes followed by the run buffer for 4 minutes. Sample was pressure injected for 5 sec at 0.5 psi. The separation voltages and buffer conditions are indicated in the figure captions. Peak heights and peak areas were calculated and plotted as required using Beckamn PACE software.

The microchip device used for trapping particles (Part II) was fabricated in Corning 0211 glass (600 µm thick, Corning Glass Co., Corning, NY) at the University of Alberta Nanofab. The weirs were etched 2 µm deep and the channels were 20 µm deep. After drilling 2 mm diameter access holes on a 600 µm thick, Corning 0211 glass cover plate, the etched substrate was bonded to it at room temperature. The side channel was used to direct 20 µm ODS beads and 200 nm $Fe_3O_4SiO_4$ nanoparticles into the chamber using in-house vacuum pressure. Fluorescence measurements were performed on a Varian Eclpise sprectrofluorimeter.

3. Results and Discussion

3.1 Capillary electrophoresis of polymeric NPs using direct LIF detection

Laser induced fluorescence (LIF) detection is ideally suited for CE. Detection limits approaching to the single molecule level have been achieved [13]. However, LIF detection usually requires derivatization of the analytes (NPs in this case) with a fluorescent probe. Iron oxide beads (1 µm dia.) labeled with Lucifer yellow (from IMI) and commercially available fluorescent 55 nm and 210 nm dia. polymeric NPs, grafted with dragon green and fluorescein respectively, were subjected to CE-LIF detection. Figure 1 shows electropherograms of the polymeric NPS. From the migration times of these two samples, it is apparent that the smaller particles migrated through the capillary faster (t_{mig} = 2.773 min) than the larger particles (t_{mig}= 3.921 minutes) under the same run conditions. However, clear separation of a mixture of the two samples was complicated by the smaller extra peaks at 2.797 minutes from the 210 nm particles co-migrating with the 55 nm particles (data not shown). From Figure 1B, it can be seen that the 210 nm particles have a peak at 1.815 min which migrates faster than the negatively charged fluorescein dye (t_{mig} = 2.513 min), and a neutral marker thiourea (t_{mig} = 2.290 minutes, detected @ 214 nm by CE-UV absorbance using the same run condition, data not shown), suggesting there is also a positively charged contaminant in the sample. From the figure it is evident that CE can be used to assess the quality of nanoparticle samples. The sample containing 55 nm beads was homogenous in size while the 210-nm sample was not.

For CE-based size characterization of NPs, it is important to validate the reproducibility of the electrophoretic mobility of the particles since this will influence the precision of the characterization. We evaluated the reproducibility of the size determination experiments by measuring the relative standard deviation (rsd) of the migration times of the 55 nm and 210 nm particles from 5 consecutive runs; the calculated rsd values were 0.9 and 1.2%, respectively. We also subjected the NPs to different separation voltages to further understand their electrokinetic behavior. As in a typical CE, the mobility varied linearly with the applied voltage, Figure 2.

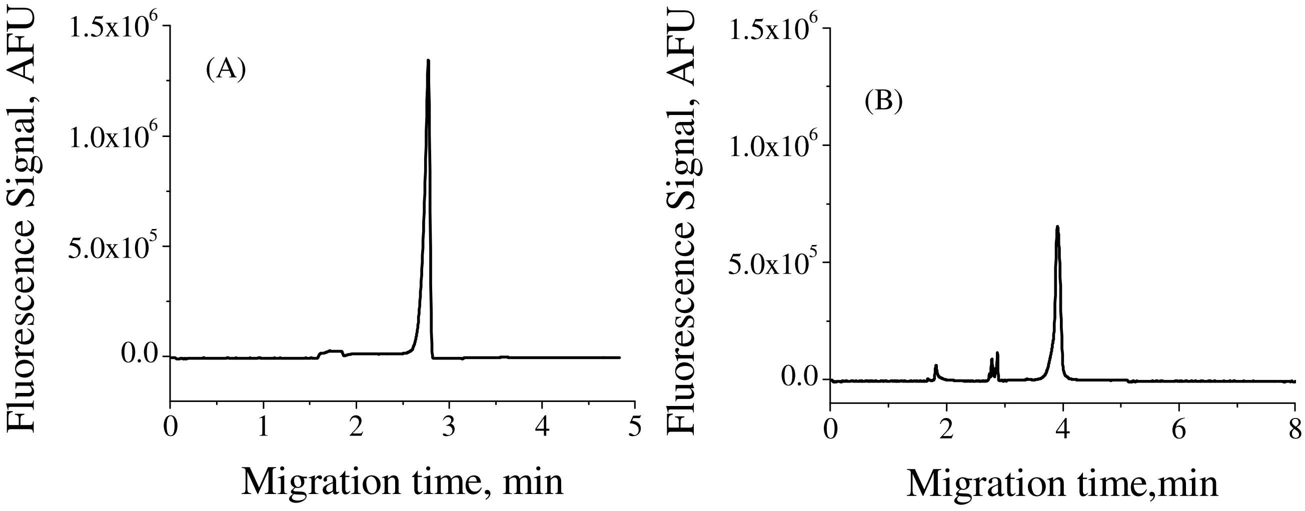

Figure 1. Electropherograms of (A) 55 nm (1.094 x 10^{14} particles/mL) polymeric NPs labeled with Dragon green and (B) 210 nm (1.965 x 10^{12} particles/mL polymeric NPs labeled with fluorescein dye. Separation was effected by applying 14 kV. The separation buffer was 50 mM Tris, pH 9.0.

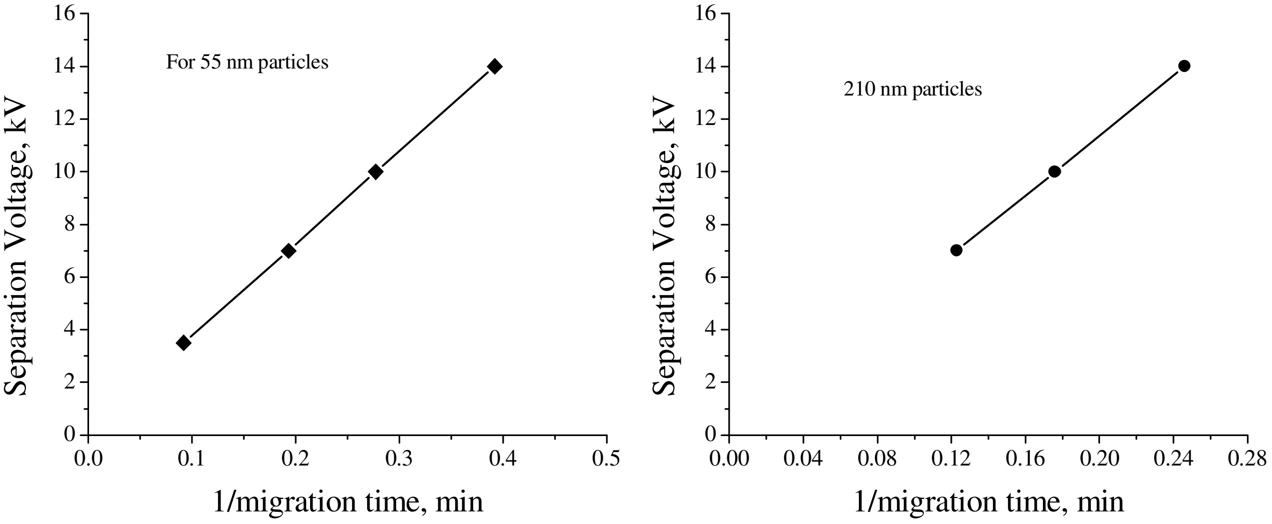

Figure 2. Effect of separation voltage on the migration times of the polymeric nanoparticles. All other experimental conditions were as in Figure 1.

1 µm beads, labeled with Lucifer yellow at IMI, were subjected to CE-LIF. Lucifer yellow dye has a similar spectrum to the thiophene fluorescent polymer used by IMI for DNA hybridization detection. The work herein provides useful and

relevant information about the conjugation chemistry used at IMI with implication to the grafting efficiency of probes onto NPs to be used in the DNA hybridization experiments. Figure 3 shows electropherograms of 1-µm Lucifer yellow-labeled beads and of the free dye in solution. In a 50 mM Tris buffer, pH 9.0, the negatively charged Lucifer yellow dye in solution gave two major peaks (Figure 3A) that have migration times of 5.876 ± 0.047 min and 6.622 ± 0.051 min (n = 4). Figure 3E shows electropherograms obtained for successively injected Lucifer yellow dye. Although the migration times of the two major peaks did not shift significantly, the intensity of the first peak decreased with the run number and several tiny peaks appeared, probably due to hydrolysis of the dye. The 1-µm Lucifer yellow-labeled bead sample also gave two major positive peaks with migration times of 5.888 ± 0.0311 min and 6.433 ± 0.0431 min, when run under the same condition as the dye sample (Figure 3B). The dips in Figure 3B could be due to unlabeled beads. Figure 3 (C and D) also shows electropherogram of a neutral electroosmotic flow (EOF) marker dye BODIPY and negatively charged fluorescein dye run under the same condition. The EOF marker has a migration time of 4.650 ± 0.018 min and fluorescein has a migration time of 5.796 ± 0.02 min.

Comparison of the migration times of the beads and the free dye shows that the Lucifer yellow dye or the chemical linkage between the beads and the dye was not stable and the major fraction of the dye was not bound to the beads. This was also confirmed by separating the beads from the supernatant solution in the sample via centrifugation and running CE-LIF of the re-suspended beads and the supernatant. The supernatant electropherograms were similar to that of Lucifer yellow dye (Figure 4). Spiking the supernatant with Lucifer yellow produced no extra peaks. The washed beads and the supernatant after 3 washes showed little signal. This confirms that most of the fluorescent signal in the bead sample arose from free Lucifer yellow dye in the bead slurry. The fluorescent spectra of the supernatant obtained on the fluorimeter also showed that the washed beads have very little signal and the supernatant showed strong fluorescence (Figure 4).

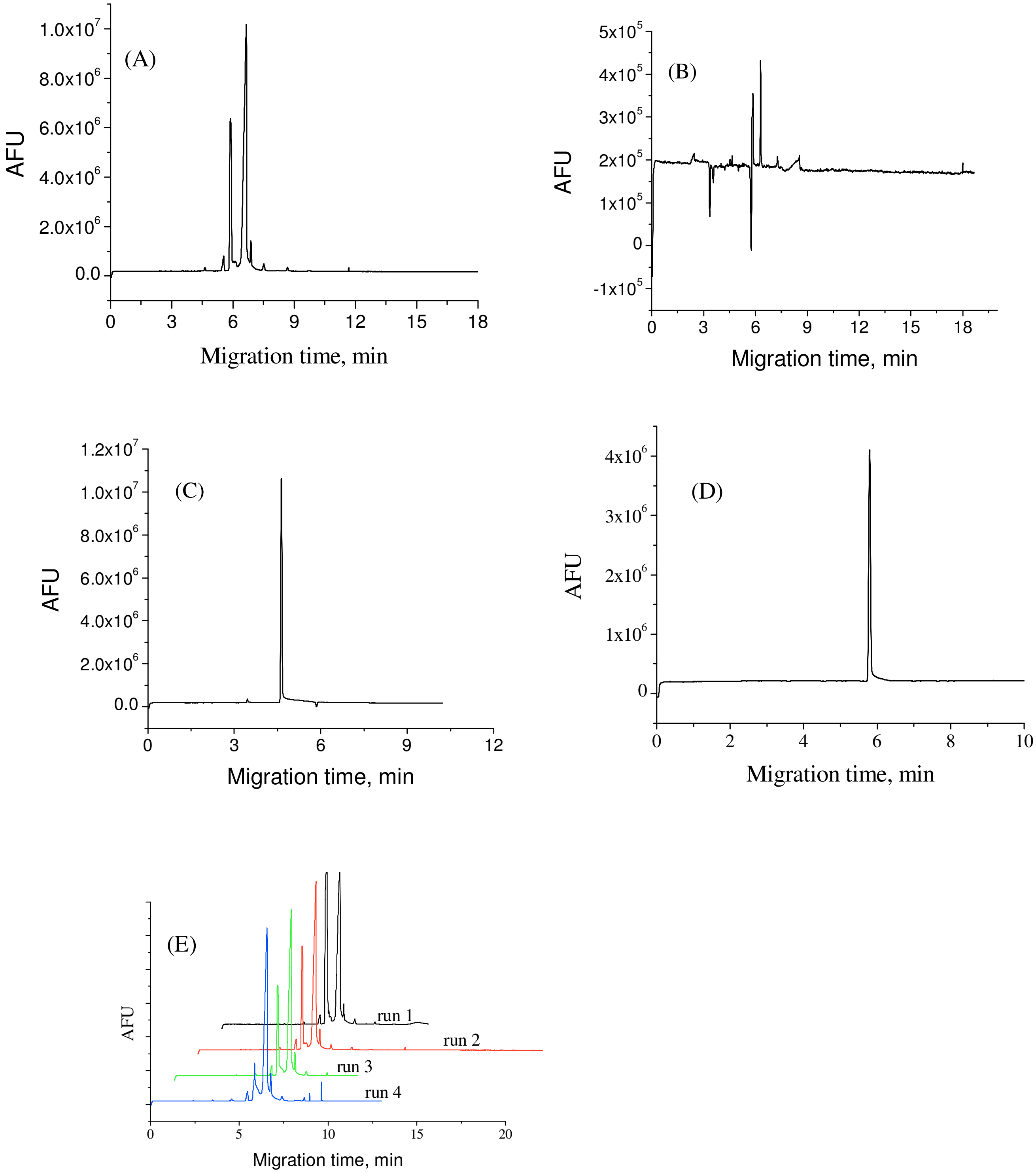

Figure 3. Electropherograms of (A) and (E) Lucifer yellow dye, (B) Lucifer yellow-labeled 1 µm beads, (C) BODIPY and (D) 50 nM fluorescein dye. CE was performed using 37 cm long, 50 mm i.d. capillary. Sample was injected for 3 sec by pressure and separation was effected by applying 7 kV. The running buffer was 50 mM Tris, pH 9.0. In (E), the X and Y axis were off-set for easy visualization.

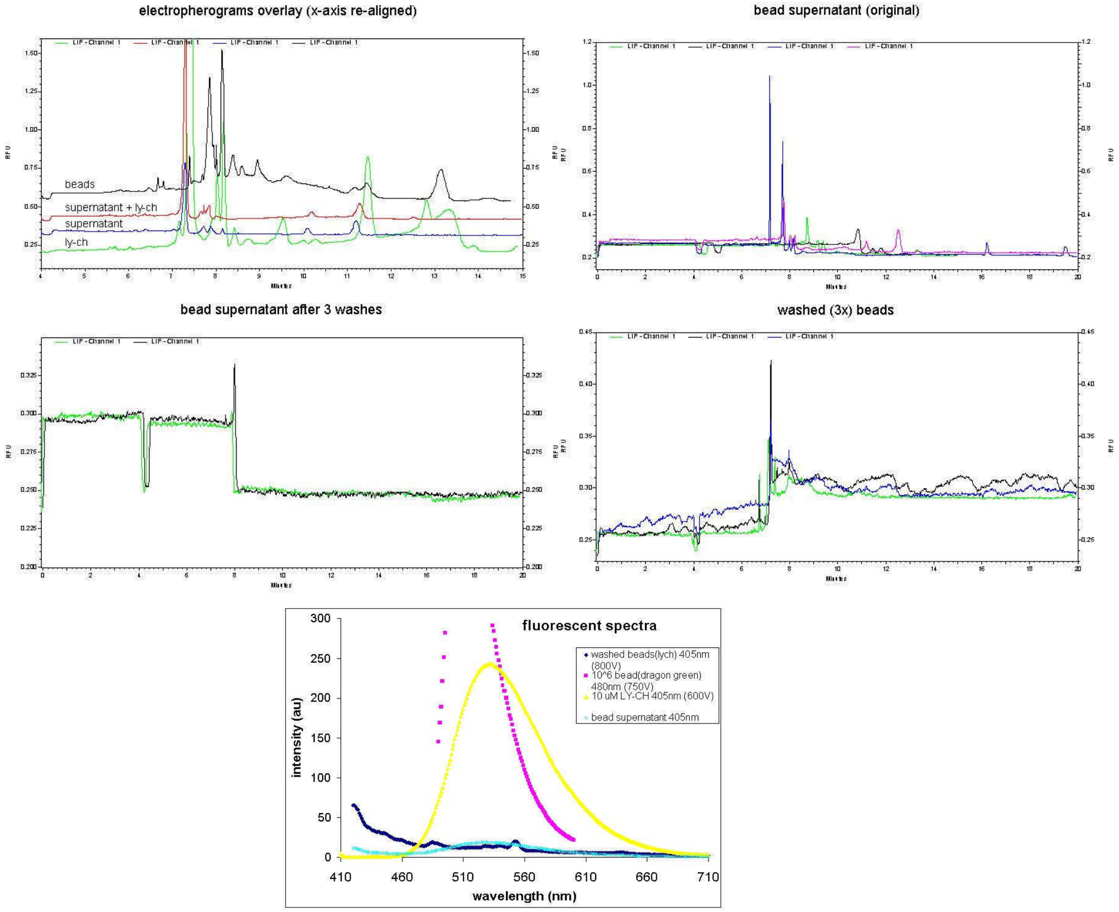

Figure 4. CE separations of beads, supernatant, supernatant spiked with Lucifer yellow, and Lucifer yellow (top left). The x-axis of the traces has been aligned for viewing. Separations of the original bead supernatant, washes, and washed beads. The fluorescent spectra (bottom) of the supernatant and washed beads all indicating that the Lucifer yellow is in free solution and not on the beads.

3.2 Capillary electrophoresis of NPs using UV absorbance detection

In order to understand the CE separation of nonfluorescent NPs, 5 nm and 20 nm gold NPs were utilized. The particles were subjected to CE separation as outlined in the experimental section. Figure 5 shows the electropherograms obtained for 5 nm gold particles and a mixture of 5 nm and 20 nm gold particles. The particles were separated according to their sizes; small particles detected first followed by the larger particles. Moreover, the purity and sharpness of the signals suggest that CE can be used to characterize the size distribution of NPs. Attempts were made to characterize the iron-oxide core NPs obtained from IMI using the same approach. However, the UV absorbances of these samples at 214 nm were too low for detection. As a result we used indirect fluorescence detection methods to characterize the NPs from IMI.

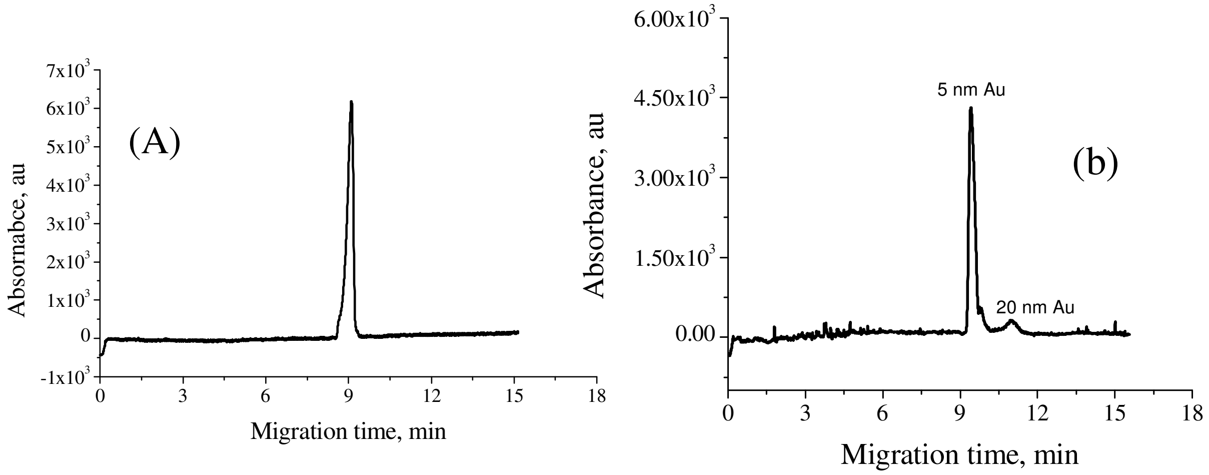

Figure 5. Electropherograms of (a) 5 nm Au nanoparticles and (b) a mixture of 5 nm and 20 nm nanoparticles. CE was performed using a 47 cm long, 75 μm i.d. capillary. Sample was injected for 5 sec by pressure and separation was effected using 15 kV. The running buffer was 50 mM Tricine, pH 8.5, buffer and detection was made at 214 nm.

3.3 Capillary electrophoresis of NPs using indirect LIF detection

Due to the absence of inherent fluorescence of the two iron-core samples (Fe_3O_4@NMe_4OH and $Fe_3O_4SiO_2$) obtained from IMI and the gold NPs, indirect LIF detection was employed to study their CE properties. The principle behind indirect LIF detection is based on the displacement of a fluorescing species present in the background electrolyte by the analyte of interest. The signal is thus derived from the buffer phase additive rather than from the analyte itself. The displacement causes a decrease in the background signal because the concentration of the fluorescent dye is lower in the eluted band compared to its steady state concentration. Thus in CE indirect LIF detection, a charged probe can be used such that the analyte ions of like charge will displace it because of the requirement of local charge neutrality, while analyte ions of opposite charge will ion-pair with it. However, it is difficult to achieve the same limit of detection for indirect LIF detection compared to direct LIF detection because noise is usually larger in the presence of a larger background signal. The theoretical limit of detection, C_{LOD}, for indirect LIF detection is given by [14],

$$C_{LOD} = C_p S_{BN}/T_R = C_p/T_R D_R$$

where Cp is the concentration of the florescent probe, S_{BN} is the relative standard deviation of the background fluorescent fluctuation (noise), T_R is the transfer ratio (the number of probe molecules displaced by one analyte molecule/particle), and D_R is the dynamic reserve (ratio of the background fluorescence intensity to the noise) .

Numerous factors must be taken into consideration when a probe is being selected for indirect LIF detection by CE. First, the spectral property of the probe must be compatible with the light source. Second, the florescent dye has to be charged and its mobility compatible to that of the analytes to minimize electrodispersion (asymmetric peaks). The probe also needs to be soluble in the buffer system. The last factor is the cost of the probe. High-purity fluorescent probes tend to be very expensive and are sold in small quantities (~5mg). The cost is usually affordable in direct LIF detection when only minute quantities of the probes are required as derivatizing agents. In the indirect CE LIF, buffers were prepared in volumes of 200-300 mL at micro-molar concentrations of fluorescent dye (fluorescein) for characterization of the NPs. Fortunately fluorescein is relatively inexpensive, unlike many of the newer fluorescent dyes. Fluorescein is negatively charged at high pH (also water soluble), and highly fluorescent at 520 nm when exited at 488 nm by argon ion laser. Gold NPs are negatively charged. To the best of our knowledge this is the first report of indirect LIF detection of NPs by CE.

Figure 6 shows electropherograms obtained for indirect LIF detection of gold NPs (10 nm dia.). The negative peak at 2.021 minutes corresponds to the gold NPs while the positive spike could be due to scattered light from the NPs. The narrow dip suggests that the in-house synthesized NPs have a narrow size distribution. In this work, we found that the peak reproducibility, however, was affected by agglomeration of the NPs over time. Figure 6B shows the signals obtained for the same NPs when the sample was vortexed for 30 sec and injected after 2.5 hr. It is known that citrate-based gold NPs undergo soft secondary aggregation. When the sample was vortexed just prior to injection the signal was highly reproducible, Figure 6c.

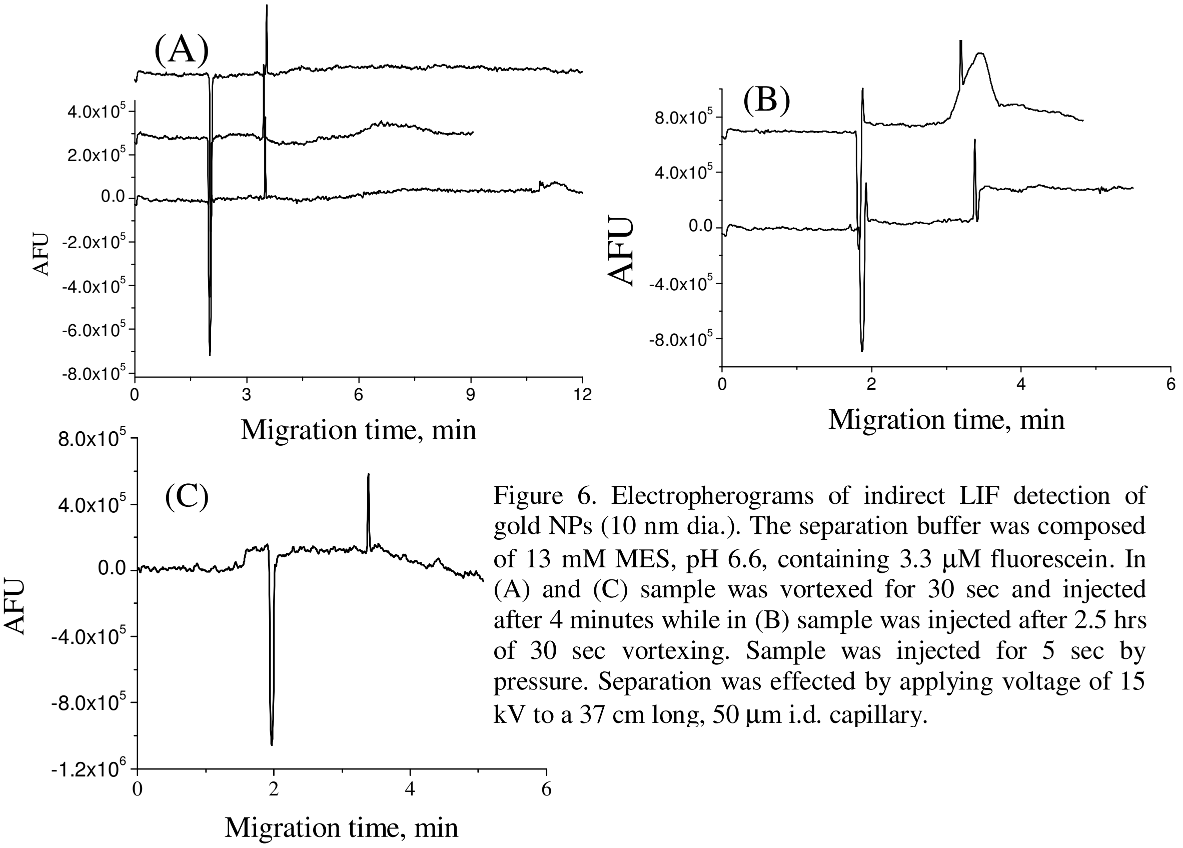

Figure 6. Electropherograms of indirect LIF detection of gold NPs (10 nm dia.). The separation buffer was composed of 13 mM MES, pH 6.6, containing 3.3 µM fluorescein. In (A) and (C) sample was vortexed for 30 sec and injected after 4 minutes while in (B) sample was injected after 2.5 hrs of 30 sec vortexing. Sample was injected for 5 sec by pressure. Separation was effected by applying voltage of 15 kV to a 37 cm long, 50 µm i.d. capillary.

Figure 7 shows electropherograms of $Fe_3O_4SiO_2$ NPs. The sharp peak indicates that the overall distribution of the electrophoretic mobility of the nanoparticles is narrow. Thus, the particles size and charge are relatively uniform. However, instead of the expected negative peak, we observed a positive peak. This could be explained as the iron core particles are positively charged and form a complex with the negatively charged fluorescein in the background buffer giving rise to a positive peak. The broad slight deep following the positive peak indicates there is a slow moving component in the sample. Direct LIF detection of the $Fe_3O_4SiO_2$ at 530 nm emission wavelength with no addition of fluorescien in the separation buffer resulted in no signals.

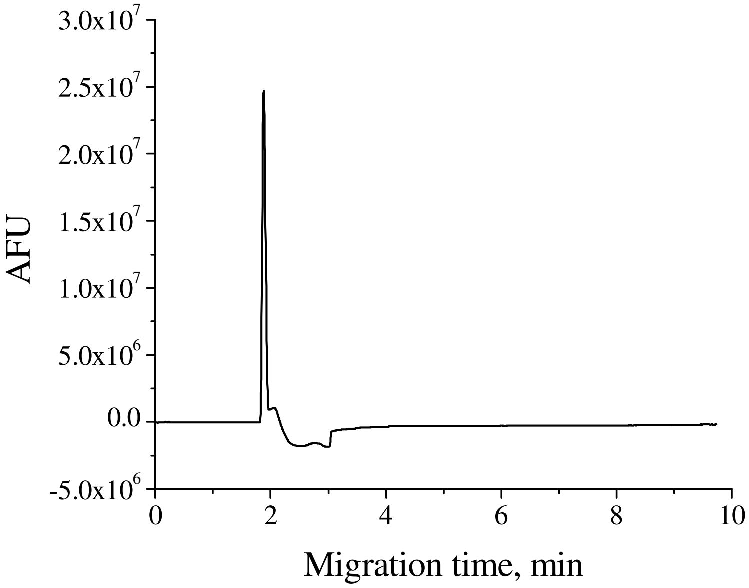

Figure 7. Electropherograms of $Fe_3O_4SiO_2$ NPs in direct LIF detection. Sample was vortexed for 30 sec, 4 minutes prior to injection. All experimental conditions are as in Figure 6.

Figure 8 shows electropherograms obtained for Fe_3O_4@NMe_4OH NPs under indirect LIF detection. Again instead of negative peaks, we observed two positive peaks in the presence of fluorescein as the background dye. Similar to the $Fe_3O_4SiO_4$ nanoparticles, we suggest that this sample also complexed with the negatively charged fluorescein probe in the separation buffer. The second peak in the figure could be due to the NMe_4^+ ions added to stabilize the particles and forming a complex with fluorescein. When the sample was successively injected without capillary wash, the migration times of the peaks increased suggesting that the EOF of the capillary was reduced due to surface modification of the capillary wall by the NMe_4^+ present in the sample. It is known that cations adsorb onto the negatively charged capillary surface, due to electrostatic attraction, causing a decrease in cathodic EOF.

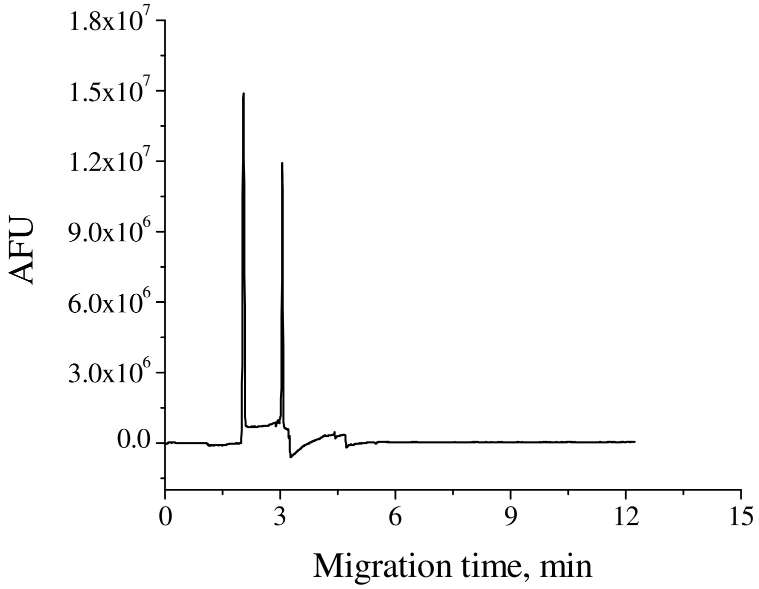

Figure 8. Electropherograms of Fe_3O_4@NMe_4OH by indirect LIF detection. Sample (directly from the sample) was injected into a 47 cm long (50 µm i.d., 360 µm o.d.) capillary by pressure for 5 sec (runs 1-3) and 2 sec (run 4). The running buffer was composed of 12 mM MES buffer, pH 6.6, and 5 µM fluorescein as background probe. Separation was effected by applying 7 kV.

When the capillary was washed with 0.1 M NaOH for 2 min followed by conditioning with the fluorescein-containing buffer for 4 minutes between runs, the EOF was regenerated and the migration times of the peaks were recovered supporting the claim above. Successive injection of the sample, with a 2 minute wash with 0.1 M NaOH followed by 4 minutes buffer conditioning in between runs, gave migration times of 2.038 ± 0.061 minutes (%RSD = 1.39, n=5) and 3.034 ± 0.089 minutes (%RSD = 2.93, n=5).

4. Conclusions

CE can be used as a means of evaluating the labeling and homodispersity of NPs. In this study we found that some of the commercially labeled nanoparticles and beads grafted at IMI showed some impurities. In particular we were quickly able to identify a NPs synthesis problem that was later resolved. The NMe_4OH used as a stabilizer for the Fe_3O_4 could potential cause problem in the DNA hybridization experiment as it modifies the microchip surface. This experiment also suggests that CE can be applied to determine the conjugation efficiency of probes and proteins to NPs. This may be of particular importance to the work IMI is undertaking to measure DNA via probe grafted on NPs.

Part II Trapping Nanoparticles in Microfluidic Devices

One of the critical areas of microfluidic processing is the interface between the microfluidic device and the macro world [1]. Sample preparation and introduction are two of the most difficult issues. The sample matrix may be incompatible with the micro size channels or the volume to be introduced into the device, at 10 μL, is too large. Typical volumes in microfluidic devices are in the nano- to pico-liter range, so microliter scales represent significant multiple volumes of a device. Furthermore limits of detection set for the project may require the full sample volume (i.e., microliters) to be processed. Therefore the sample would be pumped through the device at high flow rate to maintain rapid assay times and to process the entire sample. Such requirements can cause several problems with typical device function. Pumping fluids at high flow rates within the device may be difficult as the small channels have a significant resistance to flow. The magnetic nanoparticles become more difficult to trap as the forces acting on them are increased at high flow rates. Present day electromagnetic traps do not produce a sufficient magnetic field to extract and contain NPs. There are several possible methods to overcome this problem: increase the device volume to reduce flow rates, use larger beads that are easier to trap, and add secondary devices to aid in trapping the beads. It may also be possible to enhance the trapping of NPs pumped using a combination of electromagnetic trap and an external permanent magnet.

Larger channel volumes will negate some of the benefits to be gained from the microfluidic devices. For larger volumes processed, larger numbers of analyte molecules would be required to maintain concentrations above the limits of detection. Bead-based solid phase extraction can be used to overcome some of the above problems in microfluidic processing. The beads can be used to concentrate the sample for detection. The increased dimensions of the microfluidic devices will require more time for mass transport within the device, in particular, for the beads to capture the analyte. This requirement can be offset by the ability of larger fluidic devices to generate internal turbulent mixing.

The current microfabricated electromagnets cannot produce sufficient fields to trap the NPs against a large flow forces. Experiments at IMI and by other researchers [2] showed that as the flow rate increases, the trapping ratio (i.e. the ratio of total number of trapped beads to the total number of injected particles) decreases. Thus the problems associated with trapping NPs led to the decision to focus the IMI-lead project on the use of micron sized bead (2.8 μm in diameter) that will increase the magnetic trapping force allowing for increased flow rates and keeping the channel sizes minimal.

In the present work alternate methods to improve NP tapping were investigated. One approach followed was to use channels of different etch depths to make weirs/dams to filter the beads [3]. In this work, we fabricated a microfluidic chamber possessing “leaky” walls, Figure 1. As shown in the figure, the chamber was made by etching 20 μm deep cavity into a glass substrate, with its inlet/outlet channels obstructed by 18 μm high weirs to leave about 2 μm gap for liquid passage. Beads greater than 2 μm could thus be flushed into the chamber through a third channel and be retained behind the weirs. A similar approach for trapping NPs in a cavity is extremely challenging since the gap between the two substrates has to be in nanometer scales. Fabrication and operation of such a device would be very difficult since particles can become permanently wedged within the traps, and the constrictions increase the flow resistance of the device. Since the iron oxide NPs are much smaller than the gap in the column, we first introduced 20 μm ODS beads to occupy the first few portion of the column by applying suction to the column outlet. The beads were then immobilized by flushing the column with water for 10 minutes. Being hydrophobic, the ODS beads agglomerate in water. The $Fe_3O_4SiO_4$ NPs, in aqueous solution, were then loaded. When suction was applied, the NPs were drawn into the column and restrained by the larger ODS beads. Figure 1 shows the trapping of 200 nm $Fe_3O_4SiO_4$ particles in a microfluidics device using 20 μm ODS beads. The color of the column changed from gray to brown as the NPs were immobilized within the matrix of larger beads. The NPs filled the interstitial space of the ODS beads first and then packing progressed to fill about 1.5 cm of the 5 cm long column. Eventually it became difficult to draw more NPs into the column via suction alone as the flow rate was significantly reduced due to the tightly packed NPs. Further optimization of the packing process could allow packing longer columns with NPs with this approach.

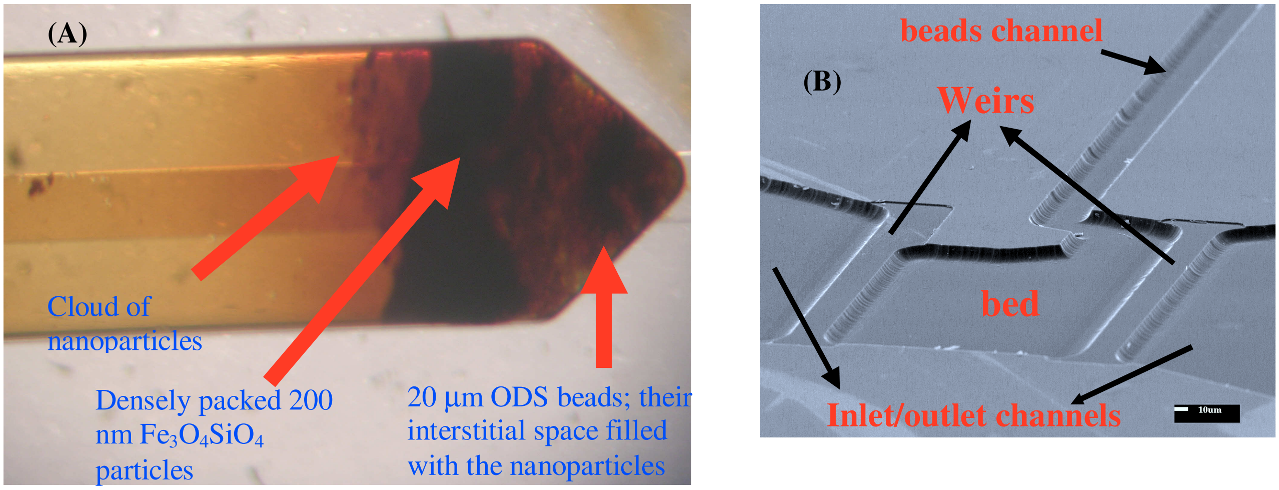
(A)
Cloud of nanoparticles
Densely packed 200 nm $Fe_3O_4SiO_4$ particles
20 µm ODS beads; their interstitial space filled with the nanoparticles
(B)
beads channel
Weirs
bed
Inlet/outlet channels
10um

Figure 1. (A) Photograph of trapped NPs using microbeads in a microfluidic device. 10 µm ODS, in methanol, were drawn into the chamber. The excess beads were then removed from the bead introduction channel and the chamber was flushed with water to agglomerate the beads. 200 nm $Fe_3O_4SiO_4$ NPs were then drawn into the chamber using house vacuum line. (B) SEM image of the microfluidic device used to produce bead-bed.

There are other approaches to trapping NPs that could be considered. A second magnetic source (a stronger permanent magnet) would provide increase field strength to immobilize and hold the particles. After trapping the permanent magnet could be removed during detection while an electromagnet would still be used on to hold the trapped particles in place. However such a device requires testing to determine if the increased field of the permanent magnet is sufficient to hold the NPs. Another approach would be to use magnetic microbeads to extract the NPs from the flow, then employ a weaker electromagnetic loop to keep the NPs in place during a stopped flow as shown in Figure 2. Likewise, this concept would require further analysis and testing.

Conclusions

The work described in Part II was carried out to support IMI in designing microfluidic devices for concentration and detection gene sequences of bacterial DNA. Elements of this research have been utilized in the follow-up CRTI 06-0187TD for a portable biological agent detection system.

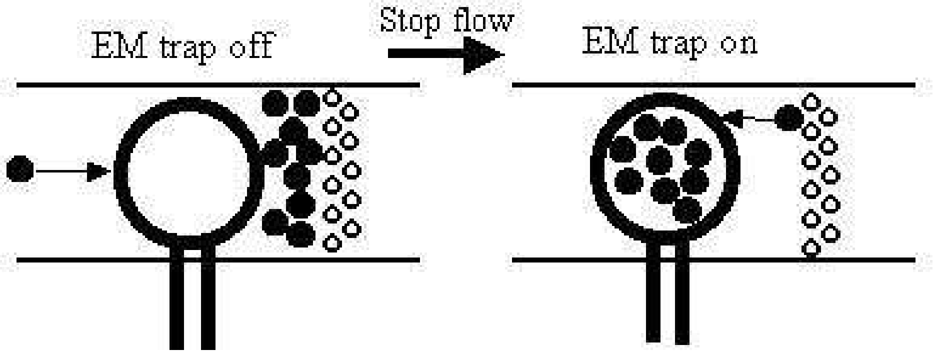

Figure 2. Filter aided magnetic capture method

References

PART I

1. M. Uhlen, *Advances in Biomagnetic Separation*, E. Hornes & O. Olsvik eds., 1994, Eaton Publ. CO. Natick.
2. J. Ugelstad, P. Stenstad, L. Kilaas, W.S. Prestvik, R. Herje, A. Berge and E. Hornes, *Review Blood Purification*, 11 (1993) 349.
3. X. Ji, S. Xu, L. Wang, M. Liu, K. Pan, H. Yuan, L. Ma, W. Xu, J. Li, Y. Bai and T. Li, *Colloids Surf. A*, 171 (2005) 257.
4. N. R. Jana, *Analyst*, 128 (2003) 954.
5. C. Nilsson, S. Birnbaum, and S. Nilsson, *J. Chromatogra. A*, 1168 (2007), 212.
6. J.P. Wilcoxon, J.E. Martin, and P. Provencio, *Langmuir*, 16 (2000) 9912.
7. W.M. Hwang, C.Y. Lee, D.W. Boo, and J.G. Choi, *Bull. Korean Chem. Soc.*, 24 (2003) 684.
8. S. P. Radko and A. Chrambach, *Electrophoresis*, 23 (2002) 1957.
9. K.H. Lin, T.C. Chu and F.K. Liu, *J. Chromatogra. A*, 1161 (2007) 314.
10. Y. H. Rezenom, A.D. Wellman, L.Tilstra, C.D. Medley and S.D. Gilman, *Analyst*, 132 (2007) 1215.
11. F.K. Liu, Y.Y. Lin and C.H. Wu, *Anal .Chim. Acta*, 528 (2005) 249.
12. U. Schnabel, C.H. Fischer and E. Kenndler, *J. Microcol. Sep.*, 9 (1997) 529.
13. Y.F. Cheng, N. J. Dovichi, *Science*, 242 (1988) 562.
14. J.P. Landers, Handbook of Capillary Electrophoresis Second Edition, CRC Press, 1996.

PART II

1. C. K. Fredrickson and Z. Hugh Fan, *Lab chip*, 2004, 4, 526.
2. Q. Ramadan, V. Samper, D. P. Poenar and C. Yu, *Biosensors and Bioelectronics*, 2006, 21, 1693.
3. A. B. Jemere, R. D. Oleschuk, F. Ouchen, F. Fajuyigbe and D. Jed Harrison, *Electrophoresis*, 2002, 23, 3537.

DOCUMENT CONTROL DATA

(Security classification of title, body of abstract and indexing annotation must be entered when the overall document is classified)

1. ORIGINATOR (the name and address of the organization preparing the document. Organizations for who the document was prepared, e.g. Establishment sponsoring a contractor's report, or tasking agency, are entered in Section 8.)

Canada West Biosciences Inc.
5429 - 60th Street
Camrose, AB T4V 4G9

2. SECURITY CLASSIFICATION (overall security classification of the document, including special warning terms if applicable)

Unclassified

3. TITLE (the complete document title as indicated on the title page. Its classification should be indicated by the appropriate abbreviation (S, C or U) in parentheses after the title).

Characterization of Nanoparticles by Capillary Electrophoresis and Trapping of Nanoparticles in Microfluidics Device

4. AUTHORS (Last name, first name, middle initial. If military, show rank, e.g. Doe, Maj. John E.)

Tang, T., Jemere, A.B., Mah, D.C.W.

5. DATE OF PUBLICATION (month and year of publication of document)

August 2009

6a. NO. OF PAGES (total containing information, include Annexes, Appendices, etc) 30

6b. NO. OF REFS (total cited in document) 17

7. DESCRIPTIVE NOTES (the category of the document, e.g. technical report, technical note or memorandum. If appropriate, enter the type of report, e.g. interim, progress, summary, annual or final. Give the inclusive dates when a specific reporting period is covered.)

Contract Report

8. SPONSORING ACTIVITY (the name of the department project office or laboratory sponsoring the research and development. Include the address.)

Defence R&D Canada – Suffield, PO Box 4000, Station Main, Medicine Hat, AB T1A 8K6

9a. PROJECT OR GRANT NO. (If appropriate, the applicable research and development project or grant number under which the document was written. Please specify whether project or grant.)

CRTI Project 03-005RD

9b. CONTRACT NO. (If appropriate, the applicable number under which the document was written.)

W7702-04R021/001/EDM

10a. ORIGINATOR'S DOCUMENT NUMBER (the official document number by which the document is identified by the originating activity. This number must be unique to this document.)

DRDC Suffield CR 2009-177

10b. OTHER DOCUMENT NOs. (Any other numbers which may be assigned this document either by the originator or by the sponsor.)

11. DOCUMENT AVAILABILITY (any limitations on further dissemination of the document, other than those imposed by security classification)

(x) Unlimited distribution
( ) Distribution limited to defence departments and defence contractors; further distribution only as approved
( ) Distribution limited to defence departments and Canadian defence contractors; further distribution only as approved
( ) Distribution limited to government departments and agencies; further distribution only as approved
( ) Distribution limited to defence departments; further distribution only as approved
( ) Other (please specify):

12. DOCUMENT ANNOUNCEMENT (any limitation to the bibliographic announcement of this document. This will normally corresponded to the Document Availability (11). However, where further distribution (beyond the audience specified in 11) is possible, a wider announcement audience may be selected).

13. ABSTRACT (a brief and factual summary of the document. It may also appear elsewhere in the body of the document itself. It is highly desirable that the abstract of classified documents be unclassified. Each paragraph of the abstract shall begin with an indication of the security classification of the information in the paragraph (unless the document itself is unclassified) represented as (S), (C) or (U). It is not necessary to include here abstracts in both official languages unless the text is bilingual).

The contractor report describes research performed for Contract No. W7702-04R-021. The work was carried out in support of CRTI 03-005RD. The report describes the use of capillary electrophoresis (CE) as an analytical method for characterizing gold, polymer and iron oxide nanoparticles (NPs). The analyte species were detected by UV/vis or laser-induced fluorescence (LIF) spectroscopy. For analytes that possessed neither UV/vis absorbance nor LIF, indirect methods of detection were employed whereby a signal-generating molecular species was added to the running buffer. NPs from a variety of commercial sources and from custom syntheses were studied. The report demonstrates that CE is a valuable tool in NP research. The report also demonstrates the feasibility of trapping nanoparticles in microfluidic devices for sample clean up and detection.

14. KEYWORDS, DESCRIPTORS or IDENTIFIERS (technically meaningful terms or short phrases that characterize a document and could be helpful in cataloguing the document. They should be selected so that no security classification is required. Identifies, such as equipment model designation, trade name, military project code name, geographic location may also be included. If possible keywords should be selected from a published thesaurus, e.g. Thesaurus of Engineering and Scientific Terms (TEST) and that thesaurus-identified. If it is not possible to select indexing terms which are Unclassified, the classification of each should be indicated as with the title.)

Microfludics, nanoparticles, capillary electrophoresis, laser induced fluorescence

Defence R&D Canada

Canada's Leader in Defence
and National Security
Science and Technology

R & D pour la défense Canada

Chef de file au Canada en matière
de science et de technologie pour
la défense et la sécurité nationale

www.drdc-rddc.gc.ca